Stratospherically induced tropospheric circulation changes under the extreme conditions of the No-Montreal-Protocol scenario

Franziska Zilker[1], Timofei Sukhodolov[2], Gabriel Chiodo[1], Marina Friedel[1], Tatiana Egorova[2], Eugene Rozanov[2,3], Jan Sedlacek[2], Svenja Seeber[1], and Thomas Peter[1]

[1]Institute for Atmospheric and Climate Science (IAC), ETH, Zurich, Switzerland
[2]Physikalisch-Meteorologisches Observatorium Davos/World Radiation Center, Davos, Switzerland
[3]St. Petersburg State University, St. Petersburg, Russia

Correspondence: Franziska Zilker (franziska.zilker@env.ethz.ch)

Abstract. The Montreal Protocol and its amendments (MPA) have been a huge success in preserving the stratospheric ozone layer from being destroyed by unabated chlorofluorocarbons (CFCs) emissions. The phase out of CFCs has not only prevented serious impacts on our health and climate, but also avoided strong alterations of atmospheric circulation patterns. With the Earth System Model SOCOLv4, we study the dynamical and climatic impacts of a scenario with unabated CFC emissions by 2100,

5   disentangling radiative and chemical (ozone-mediated) effects of CFCs. In the stratosphere, chemical effects of CFCs (i.e. the resulting ozone loss) are the main drivers of circulation changes, weakening wintertime polar vortices and speeding up the Brewer-Dobson circulation. These dynamical impacts during wintertime are due to low-latitude ozone depletion and resulting reduction of the equator-to-pole temperature gradient. In Southern Hemisphere (SH) summer, the vortex strengthens, similar due to the effects of the Antarctic ozone hole over the second half of the 20th century. Furthermore, the winter and spring

10 vortex variability increases in the SH, whereas it decreases in summer and fall. This seasonal variation of wind speed in the stratosphere has regional implications on the tropospheric circulation modes. We find coherent changes in the troposphere, such as negative Southern Annular mode (SAM) and North Atlantic Oscillation (NAO) during seasons with a weaker vortex (winter and spring); the opposite occurs during seasons with stronger westerlies in the stratosphere (summer). In the troposphere, radiative heating by CFCs prevails throughout the year, shifting the SAM into a positive phase and canceling out the ozone-

15 induced effects on the NAO. Furthermore, global warming is amplified by 1.9 K with regionally up to 12 K increase over Eastern Canada and Western Arctic. Our study sheds light into the adverse effects of a non-adherence to the MPA on the global atmospheric circulation, uncovering the roles of the underlying physical mechanisms. In so doing, our study emphasizes the importance of the MPA for Earth's climate, to avoid regional amplifications of negative climate impacts

1   Introduction

20 The emission of anthropogenic halogenated ozone depleting substances (hODSs) has been predominantly responsible for stratospheric ozone depletion since the 1960s (Solomon, 1999). As a result, the Montreal Protocol and its amendments and adjustments (MPA) were ratified to phase out global ODS production and consumption (World Meteorological Organization, (WMO), 2022). The MPA mitigated severe health impacts from harmful UV radiation and negative climate impacts (Barnes

et al., 2019; Neale et al., 2021). It has been also recently shown that the MPA restrictions led to clear changes in vertical
25 dynamical coupling between the stratosphere and the troposphere in past decades with implications for the tropospheric circu-
lation modes (Banerjee et al., 2020). Unlike the health and climates impacts, such circulation response to much stronger future
effects of avoided CFC emissions has not been widely addressed.

As already known from historical ozone depletion, the influence from stratospheric circulation changes on the troposphere
and surface can be considerable, especially in the SH (Thompson and Solomon, 2002; Gillett and Thompson, 2003; Thompson
30 et al., 2005). The Antarctic ozone hole caused polar stratospheric temperatures to decrease (through reduced absorption of
solar radiation) by up to 12 K until the end of the 20th century (Randel et al., 2016; Calvo et al., 2017). As a consequence, the
equator-to-pole temperature gradient intensified, which in turn strengthened the polar vortex and caused a delay in its break-up
in spring (e.g. Thompson and Solomon, 2002; Dennison et al., 2015). The large-scale SH tropospheric circulation responded to
the stronger vortex with a poleward shift of the mid-latitude (eddy-driven) jet stream, a positive trend in the Southern Annular
35 Mode (SAM), an expanding Hadley cell and a subsequent expansion of the subtropical dry zone (Banerjee et al. (2020) and
references therein). In the Northern Hemisphere (NH), the tropospheric and surface response to ozone depletion is less well
established, partly because long-term trends in Arctic ozone are much smaller than in the Antarctic (Karpechko et al., 2018).
However, model simulations (Calvo et al., 2015) and observations (Ivy et al., 2017) show that in individual years with strong
ozone depletion in the Arctic, the Northern Annular Mode (NAM) shifts to a positive phase in spring, and ozone has been
40 shown to play a sizable role in this link (Friedel et al., 2022). Arctic ozone can also affect tropospheric climate in a scenario
with large CO2 forcing (Chiodo and Polvani, 2019). Overall, the historical ozone depletion period showed that CFCs have the
potential to severely alter the stratospheric state via the ozone depletion they induce, and in turn triggered sizable changes in
the large-scale tropospheric circulation.

In the "world avoided" (a world without the restriction of the MPA (No-MPA) and thus a continued unabated increase
45 of CFCs throughout the 21st century), the coupling between the stratosphere and the troposphere would become stronger
(Morgenstern et al., 2008). In the scope of this study we will focus on the changes of the polar vortices that have a direct effect
on the tropospheric circulation, mostly regarding the dominant modes of tropospheric mid-latitude variability, the Northern
and Southern Annular Modes (NAM/SAM) and the North Atlantic oscillation (NAO).

Some previous "world avoided" modeling studies are not fully interactive and have limited representation of tropospheric
50 and surface processes (e.g. fixed tropospheric ozone in Newman et al. (2009), fixed sea surface temperatures and sea ice in
Egorova et al. (2013) or "prescribed atmospheric chemistry effects" Goyal et al. (2019)) and only briefly touched upon how
the changes in the stratosphere affect the large-scale tropospheric circulation. Stronger polar vortices and a strengthening of
the SAM with respect to the present day would be detectable by 2030 (Morgenstern et al., 2008). Newman et al. (2009)
showed that the upper flank of the subtropical jet (30° N, 70 hPa) would significantly strengthen by 2065. Using a similar
55 forcing, Egorova et al. (2013) reported a substantial weakening of the polar vortices and a shift of the Northern Annular Mode
(NAM) to a negative phase by 2100. This shift is consistent with what we know on how the stratosphere and troposphere
are dynamically coupled (Kidston et al., 2015; Domeisen and Butler, 2020). A weakening of the stratospheric polar vortex
leads to an equatorward shift of the tropospheric mid-latitude jet and is associated with a negative phase of the North Atlantic

oscillation (NAO) and NAM/SAM. The equatorward shift of the storm tracks goes along with anomalous surface temperature
60   patterns. In the case of a negative NAO pattern, there is a warming over Eastern Canada and cooling over northern Eurasia. In
contrast, an intensification of the polar vortex leads to the opposite effect: a poleward shift of the tropospheric mid-latitude jet
and a positive SAM and NAO index, making the storm tracks stronger and more zonally oriented towards the pole (Kidston
et al., 2015; Domeisen and Butler, 2020). In general, similar mechanisms may also be at work in the case of ozone depletion
from unabated CFCs, but the sign and details of these mechanisms remain unclear in the context of world-avoided scenario
65   studies.

In addition to their role in destroying ozone, CFCs are important greenhouse gasses (GHGs), and can thus directly affect
surface temperature by trapping infrared radiation. Goyal et al. (2019) state that the MPA avoided around 1 K global warming
by 2050, Garcia et al. (2012) find a 2.5 K increase in global surface temperature by 2070, whereas Egorova et al. (2013) see only
significant surface warming of up to 1 K over the South Pole and Southern China and up to -2.5 K regional cooling in Eurasia
70   and Argentina in 2100. In their most recent study, Egorova et al. (2013) report a surface warming of 2.5 K by 2100. However,
to which degree CFCs have an impact on surface warming (via long-wave trapping) or can be potentially offset by cooling
resulting from ozone depletion is still controversially discussed (Velders et al., 2007; Goyal et al., 2019; Morgenstern et al.,
2020; Chiodo and Polvani, 2022; Morgenstern et al., 2021). Taken together, the climatic impacts of unabated CFC emissions,
in particular the role of direct (GHG) and ozone-mediated effects, remain poorly understood.

75   In this study, we complement Egorova et al. (2022), who examine the impacts of a No-MPA scenario at the end of the
century with an Earth System Model focusing on the ozone layer, surface air temperature, sea-ice cover, and precipitation. We
shed light on the mechanisms, by investigating how ozone depletion (section 3.1) changes the stratospheric circulation in a
No-MPA scenario (3.2) and how these changes manifest at the surface in the SH (3.3) and in NH winter (3.4) and how surface
temperatures are affected (3.5) at the end of 21st century with the fully interactive Earth System Model SOCOLv4. We also aim
80   to disentangle the impacts of stratospheric ozone depletion on the surface from the warming effect of abundant CFCs. Using
such an extreme scenario allows for a very clear signal-to-noise ratio of the modeled response without the need for advanced
statistical analysis.

2   Method

The Earth System Model (ESM) SOCOLv4.0 (Sukhodolov et al., 2021) was used to conduct the set of free-running experiments
85   to distinguish between chemical (i.e. ozone-mediated) and radiative CFC contribution in the No-Montreal-Protocol scenario.
SOCOLv4.0 consists of the interactively coupled Earth System Model (MPIMET, Hamburg, Germany) (Mauritsen et al.,
2019), the chemistry module MEZON (Egorova et al., 2003) and the sulfate aerosol microphysical module AER (Weisenstein
et al., 1997; Feinberg et al., 2019) and, thus, includes most of the known atmospheric processes involved in the ozone net
chemical production and transport as well as its feedbacks with climate. Each experiment consists of three-member ensemble
90   simulations with MPA (ref) and without MPA (noMPA) limitations, covering the period 1980-2100. The model boundary
conditions mostly follow the recommendations of CMIP6 under the historical (1980-2014) and SSP2-4.5 (2015-2100) emission

scenarios (Riahi et al., 2017). In the noMPA experiment, hODS surface mixing ratios have been increased by 3 % per year since 1987 (Velders et al., 2007) for regulated species. For unregulated species, we follow the recommendations of World Meteorological Organization (WMO) (2018) (see Egorova et al. (2022) for details). Throughout the study, we refer to hODS as CFCs.

95

To distinguish between the direct greenhouse effect of CFCs and their chemical effects (i.e ozone depletion), we have performed an additional model run, where increasing CFCs were active only chemically but not radiatively (the CFC fields of the ref run were prescribed in the radiation scheme) under SSP2-4.5. See Table 1 for further details.

In the results and discussion we mainly focus on the months June, July and August (JJA), where the signal is most prominent,
100 to discuss the mechanisms. Results for other seasons are shown in the supplemental material. In all figures (if applicable) statistical significance is calculated similarly to a two-sided t-test at a 90 % confidence level following Gutiérrez et al. (2021) and all not statistically significant areas are stippled. Unless indicated differently, all figures show the ensemble mean.

Table 1. List of experiment simulation procedure (left) and investigated effects (right). All experiments were performed with the SSP2-4.5 scenario.

Experiment	Simulation procedure		Effect
noMPA_CFCRadOff	– MPA not in place		**CFC chemical effect**:
	– CFCs inactive for radiation		noMPA_CFCRadOff − ref
	– 1 member 120 years		
	– 2 members branched out after 2070 and		**CFC radiative effect**:
	simulated for 30 years		noMPA− noMPA_CFCRadOff
noMPA	– MPA not in place		**Total effect**: noMPA − ref
	– CFCs active for radiation		
	– 1 member 120 years		
	– 2 members branched out after 2010 and		
	simulated for 90 years		
reference (ref)	– MPA in place		
	– 3 members 120 years		

3 Results

3.1 Ozone under the No-Montreal-Protocol scenario

105 First, we analyze the impact of a hypothetical No-MPA scenario on ozone and the subsequent variations of stratospheric temperature and zonal winds due to ozone changes. In the second part, we investigate how the (ozone-driven) stratospheric circulation changes as well as the impact of CFCs are linked to the tropospheric large scale circulation and the surface.
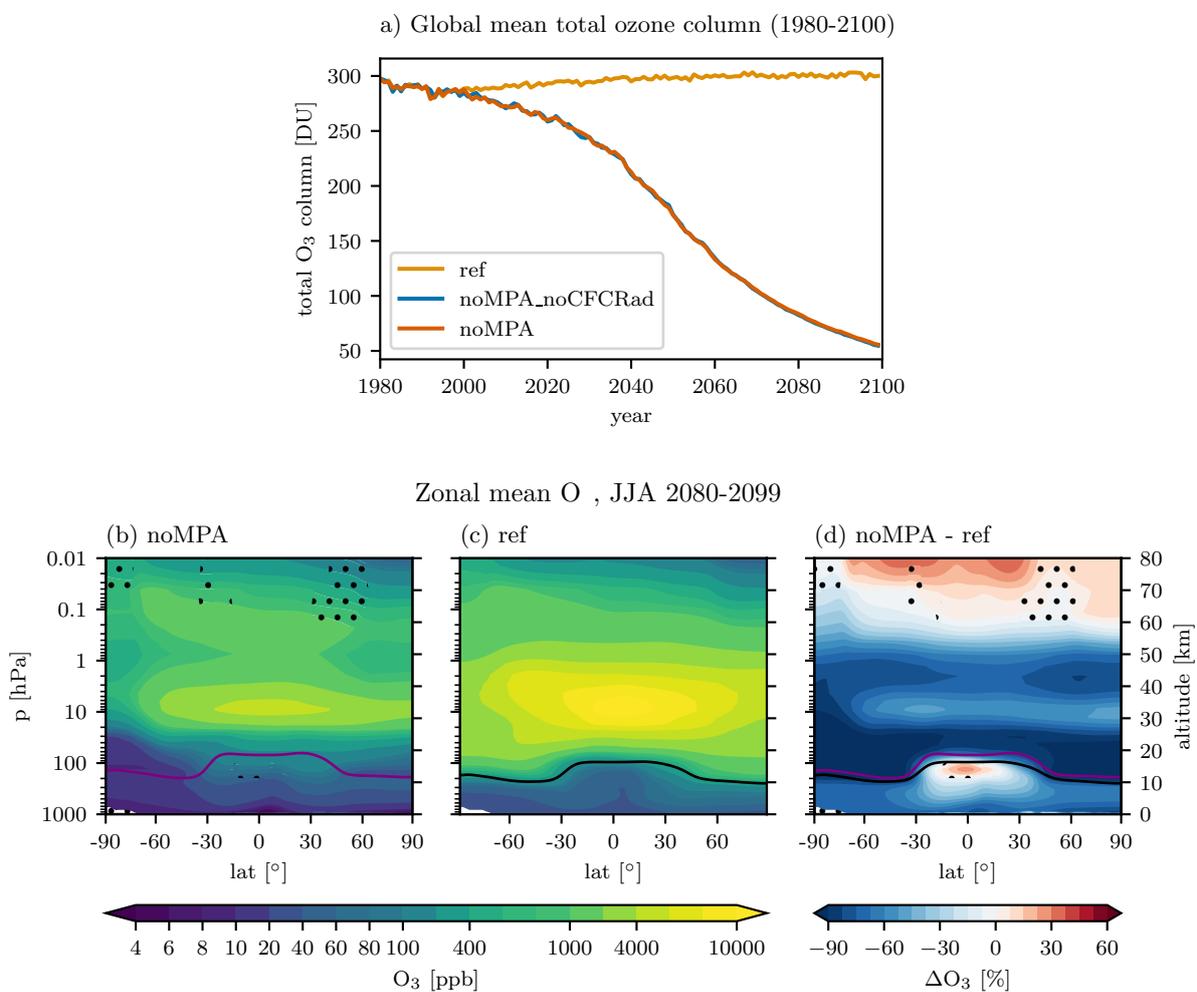

Figure 1. Top: Global mean total ozone column evolution from 1980-2099 for the reference, noMPA and noMPA_noCFCRad scenarios. Bottom: Zonal mean ozone noMPA (b), ref (c) and differences in % of noMPA−ref (d) for JJA 2080–2099. The tropopause height is indicated in purple for the noMPA and in black for the MPA reference experiment. Stippling indicates not significant at a 90 % confidence level. Colorbar levels for b and c are evenly numbered in log spacing.

In a scenario where the MPA is not in place, the abundant CFCs in the atmosphere severely reduce the global total ozone column to only 60 DU by the end of the 21st century in both No-MPA experiments (Fig. 1a). Note that both No-MPA scenarios are lying on top of each other, suggesting that radiative effects of CFCs alone do not affect the global ozone content. This severe ozone reduction is consistent with findings from e.g. Garcia et al. (2012), who reported a collapse of the global ozone layer with ozone columns below 100 DU in a No-MPA scenario in the mid 21st century (see also e.g. Goyal et al. (2019); Velders et al. (2007); Newman et al. (2009); Egorova et al. (2013, 2022); Young et al. (2021)). Figure 1 (bottom) shows the zonal mean ozone of the world without a Montreal Protocol (noMPA, b) compared to the reference (c) and the difference (noMPA-ref) (d) at the end of the century for austral winter (JJA). The uncontrolled CFC emissions have increased the chlorine concentration by a factor of 20-80 compared to the reference at the end of the 21st century, which causes an ozone depletion by up to 90 % in the stratosphere, with the strongest reduction happening in the lower stratosphere. Gas-phase ozone destruction by chlorine is additionally accelerated by its heterogeneous activation on stratospheric aerosols and polar stratospheric clouds (PSCs), which also became much more widespread due to temperature drop in the lower stratosphere (Fig. 2a, c). The cooling is especially prominent in the tropical lower stratosphere, where temperatures drop below the PSC Type 1 formation threshold of 195 K between 130 and 20 hPa (Fig. 2c) and Cl_2 (Fig. 2b, d) accumulates. This was also observed in Newman et al. (2009); Garcia et al. (2012) and we also see an increase of PSC Type 1 (nitric acid trihydrate (NAT) and supercooled ternary solution (STS)) (Fig. 2a) in the tropics. PSCs Type 2 (ice crystals, when temperatures fall below 190 K) are only allowed down to 50° in the NH and SH in SOCOL.
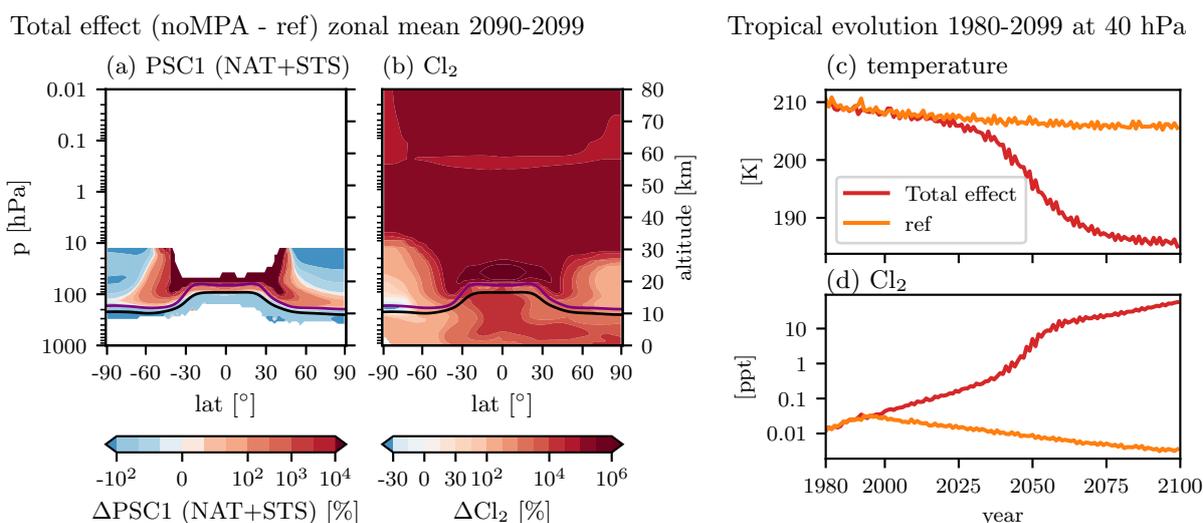

Figure 2. Left: 2090-2099 annual mean zonal mean of PSC Type 1 (nitric acid trihydrate (NAT) and supercooled ternary solution (STS)) (a) and Cl_2 (b) differences in % for the total effect (noMPA−ref). The tropopause height is indicated in purple for the noMPA and in black for the MPA reference experiment. Colorbar levels for (a) and (b) are linear around 0 and log spacing < -10 % and > 10 % for (a) and > 30 % for (b). Right: Evolution of tropical mean (23° N – 23° S) temperature (c) and Cl_2 (d) anomalies at 40 hPa from 1980 to 2099 for the total effect (noMPA-ref). Note that (d) has a log y-axis.

125   In the troposphere, ozone is depleted by up to 60 % consistent with the documented impacts of ODS on tropospheric ozone
via e.g. changes in stratosphere-troposphere exchange (Banerjee et al., 2016; Shindell et al., 2013). At around 100 hPa in low
latitudes, self-healing of the ozone layer occurs (Fig. 1d). With depleted ozone in high altitudes, UV radiation can penetrate
further down and produce ozone there, as it is also observed in Morgenstern et al. (2008); Egorova et al. (2013, 2022). In the
No-MPA scenario at the end of the 21st century, ozone depletion is no longer subject to any season or restricted to the polar
130   regions, but is happening globally all year round (Fig. A1).

3.2   Stratospheric response

Here, we investigate the effect of the No-MPA scenario in JJA on zonal mean temperatures (Fig. 3c), zonal winds (Fig. 3
f) and age of air (Fig. B1c) and go into the decomposition of the CFC chemical (Fig. 3a, d) and radiative effect (Fig. 3b,
e) to investigate the processes and quantify their contributions to the total impact of No-MPA. Consistent with other "world
135   avoided" studies (e.g. Goyal et al., 2019; Garcia et al., 2012), the global ozone depletion at the end of the 21st century leads
to a severe decrease in lower stratospheric temperatures. Fig. 3c shows the temperature response to the combined effect of the
CFC chemical effect (ozone depletion), which mainly cools the stratosphere, and the CFC radiative effect, which warms the
troposphere and parts of the stratosphere. Lower stratospheric temperatures (100–20 hPa) drop by over 20 K and by over 30 K
in the upper stratosphere (3–0.7 hPa) as shown in Fig. 3a. This is coherent with the pattern of ozone anomalies induced by
140   CFCs (Fig. 1d), indicating that the cooling is mostly due to reduced shortwave absorption of solar radiation by ozone (Fig. 1a,
d). The cooling is especially prominent in the tropics (Fig. 3a, c), where heterogeneous chlorine activation enhances ozone
destruction (Fig. 2a, b). This severe cooling is seen throughout all seasons (Fig. C1). The area of reduced cooling between
20–3 hPa in the tropics and NH can be explained on the one hand by the maximum ozone concentration region at around
10 hPa (see Fig. 1b and c) and on the other hand by the increased absorption of infrared radiation at 9.6 μm as missing ozone
145   allows this radiation to penetrate higher up (Chipperfield and Pyle, 1988; Shine, 1986).

The drastic temperature changes in the stratosphere alter the lapse rate (Fig. D1) in the "world avoided" scenario, lifting
the tropopause in the tropics, which was also observed by Newman et al. (2009). The upward shift in the tropical tropopause
(reaching 50 hPa) is almost entirely due to ozone depletion, with CFC radiation barely affecting it as seen in Figures 3b and
D1. This effect is similar to the tropopause rise from well-mixed GHG (Santer et al., 2003; Meng et al., 2021). Above the
150   tropopause, the stratospheric temperatures strongly increase up to the inflection point at 3 hPa, where they start to decrease
again, suggesting that the stratopause drops to lower altitudes in the No-MPA experiments shrinking the stratosphere compared
to the reference.

Interestingly, the Antarctic stratosphere also exhibits a warming of over 3 K at around 10 hPa (similar signal for Arctic
stratosphere in Fig. C1d and f). Newman et al. (2009) explained it by an increased downwelling due to the Brewer-Dobson
155   circulation (BDC) speed-up. However, CO changes shown in Fig. B1d and f, indicate reduced vertical transport from the meso-
sphere. A similar warming has also been observed under ozone hole conditions by Ball et al. (2016) using nudged historical
simulations and Calvo et al. (2017); see their Fig. 1b), although the warming at these altitudes is not significant. The warming
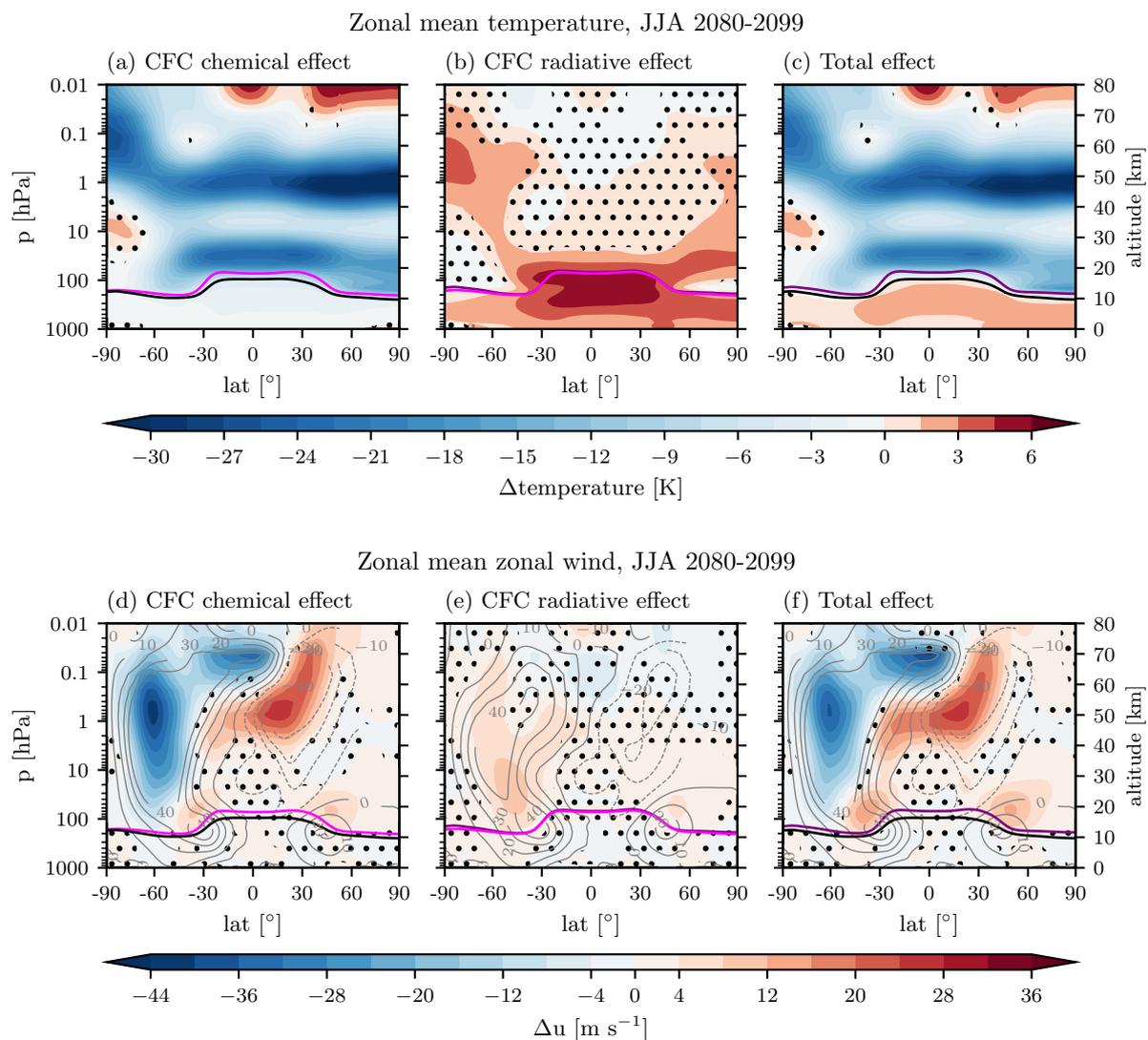
Figure 3. Zonal mean temperature differences (upper row) and zonal mean zonal wind differences (bottom row) for JJA 2080-2099. The left column shows CFC chemical effect (noMPA_CFCRadOFF−ref), the center column the CFC radiative effect (noMPA−noMPA_CFCRadOFF) and the right column the total effect of CFC chemical and CFC radiative effect combined (noMPA−ref). The tropopause height is indicated in purple for the noMPA, in magenta for noMPA_CFCRadOff and in black for the reference experiment. Stippling indicates not significant at a 90 % confidence level. For zonal wind in the bottom row, the contour lines indicate the ref zonal wind profile. Note that the color saturation for temperature (top row) is different for negative and positive values.

at 10 hPa could then also be partly explained by the weaker vortex, allowing warmer air from the mid-latitudes to be mixed into the polar stratosphere more easily.

160   CFCs by themselves (i.e. without considering their effects on ozone, Fig. 3b) strongly warm (by up to 5 K) the troposphere, consistent with previous studies (Garcia et al., 2012; Goyal et al., 2019); we will examine this feature, along with surface temperature in more detail in section 3.5. The CFC-induced warming also extends into the lower stratosphere up to 20 hPa, which is consistent with the recent findings of Chiodo and Polvani (2022), indicating that this is a direct (radiative) effect, without any influence of dynamical changes in this region. Upper stratospheric warming at high latitudes in Fig. 3b most likely

165   stems from the BDC speed-up (see later this section).
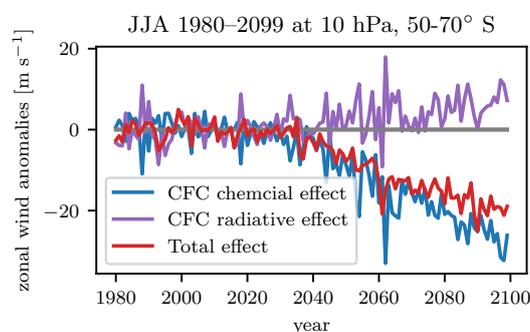
Figure 4. Zonal wind evolution at 10 hPa 50–70° S for the CFC chemical effect (noMPA_CFCRadOFF − ref), the CFC radiative effect (noMPA − noMPA_CFCRadOFF) and the total effect of CFC chemical and CFC radiative effect combined (noMPA − ref).

    Next, we aim at understanding in more detail the dynamical impacts of a No-MPA scenario. In Fig. 3f the zonal wind response to the overall CFC effect is depicted. The wintertime polar vortex speed reduces substantially, whereas the subtropical jets (STJs) shift up and accelerate in both hemispheres. Furthermore, the BDC also speeds up, as the age of air gets younger in the entire stratosphere (Fig. B1c).

170   As seen in Fig. 2c, the missing shortwave absorption from depleted ozone starts to reduce tropical temperatures in the lower stratosphere by 2030 and causes them to drop to 185 K by 2090. This severe cooling in the tropics reduces the equator-to-pole temperature gradient (Fig. 3a). This reduction in the gradient is largest in the SH winter and starts to weaken the polar cap zonal wind at 10 hPa by 2040 (blue and red lines in Fig. 4). Consequently, the polar vortex slows down due to the severe cooling of the tropical lower stratosphere (around 50 hPa in Fig. 3a) from the CFC chemical effect, i.e. ozone depletion. At the end of

175   the 21st century, the polar vortex in the SH has significantly slowed down by up to 25 m s^{-1} at 10 hPa and 40 m s^{-1} at 1 hPa (Fig. 3d). In the NH, we find a slowdown of the vortex by up to 15 m s^{-1} at 10 hPa, although this signal is limited to individual seasons such as fall, winter and spring (Fig. E1). Egorova et al. (2013) observe a similar weakening of the polar vortices. For summer, we observe the opposite effect in both hemispheres. The stratospheric winds strengthen (Figures E1d for SH and 3d for NH summer) due to stronger polar cooling than in winter, which increases the equator-to-pole gradient again (Figures C1d

180   for SH and 3a for NH summer).

    Compared to the CFC chemical effect, we see that the polar vortices are slightly stronger by up to 10 m s^{-1} in the SH (Fig. 3e) and NH during winter (Fig. E1e) for the CFC radiative effect. This enhancement originates from the CFC warming in

the tropical troposphere and lower stratosphere. Therefore the equator-to-pole temperature gradient in the lower stratosphere is larger when the CFC warming scenario is included. This is also seen in the SH polar cap wind evolution (purple line Fig. 4).

185 Additionally, we observe a strengthening of the upward flank of the subtropical jets near the tropopause and poleward shift (around 3° N/S) of the STJs throughout all seasons and scenarios (Figures 3 bottom row and E1). Polar lower stratospheric cooling during summertime further contributes to these dynamical changes, acting in the same way as Antarctic ozone hole conditions (e.g. Previdi and Polvani, 2014).

As a consequence of the weaker vortices and the stronger STJs, planetary waves can more efficiently propagate to the strato-
190 sphere. There they induce an acceleration of the Brewer Dobson circulation, leading to a decrease in age of air (AoA) in the global stratosphere (Fig. B1 top row), consistent with previous studies (Egorova et al., 2013; Newman et al., 2009; Morgenstern et al., 2008). Here, we find that this strengthening is almost entirely due to CFC-induced ozone depletion (Fig. B1a), similar to what occurred in the recent past (Abalos et al., 2019; Polvani et al., 2019). The strongest effect is on the shallow branch of the BDC, where the air gets younger by up to 0.8 years. The radiative heating by CFC further contributes to the speedup of
195 the BDC, (reduction by 0.3 years, mainly the deep branch, Fig. B1b), leading to a total AoA decline by 0.5 years in the deep branch and to more than a year in the shallow branch (Fig. B1c).

In summary, the severe cooling from missing ozone has substantial implications for the stratospheric circulation, which, depending on the season, are the opposite to the historic ozone depletion period (winter) or show the same sign (summer).

3.3 Implications on SAM

200 To better understand the stratospheric implications of the No-MPA scenarios on the tropospheric variability modes, we focus on the SH polar vortex and SAM. SAM is a large-scale climate pattern in the SH with implications for temperature and precipitation. Figure 5 (upper row) shows the seasonal cycle of zonal wind changes between 40–70° S. As described in section 3.2, the winter time polar vortex substantially slows down due to the CFC chemical effect. (Fig. 5a, c). This weaker vortex in turn becomes more variable in winter and beginning of spring (Fig. 5d), as wave propagation into the stratosphere is facilitated,
205 which increases the likelihood of Sudden Stratospheric Warmings (SSW). Morgenstern et al. (2022) showed that SOCOL is among the models able to generate SSWs in the SH. The weaker vortex in winter and spring manifests in the troposphere by pushing the tropospheric SAM to a more negative phase (Figures 6a, winter, F1a, spring). In contrast, winds in the stratosphere strengthen in summer and fall, thus shifting the SAM to a more positive phase (Figures 6d, F1d). The tropospheric circulation response to the different vortex regimes is consistent with what is known about the effects of the polar vortex on the
210 tropospheric circulation (e.g. Domeisen and Butler, 2020).

For the CFC radiative effects, the opposite happens: The vortex strengthens in all seasons, causing a shift of the SAM to a more positive phase (SAM+) all year round (Fig. 6b, e, F1b, e). Additionally, the vortex variability decreases. Combining both CFC effects shows (Fig. 6c, f, F1c, f) that the SAM+ response is dominated by the CFC radiative effect. It is only slightly reduced where the SAM is in a negative phase due to the CFC chemical effect (summer and spring), but reinforced where
215 chemical and radiative CFC effects contribute to the positive phase (winter and fall).

These findings are consistent with changes in wind at 500 hPa, which we use as a proxy for the eddy-driven jet (Fig. F2). Most remarkably, the strongest response in the eddy-driven jet is seen in austral summer (DJF), when the jet strongly contracts poleward in the SH (Fig. F2c); this is due to the fact that during this season, chemical and radiative effects of CFCs act in the same direction, much in the same way as GHGs and the ozone hole affected the westerly winds in the recent past (e.g. Previdi 220 and Polvani, 2014).
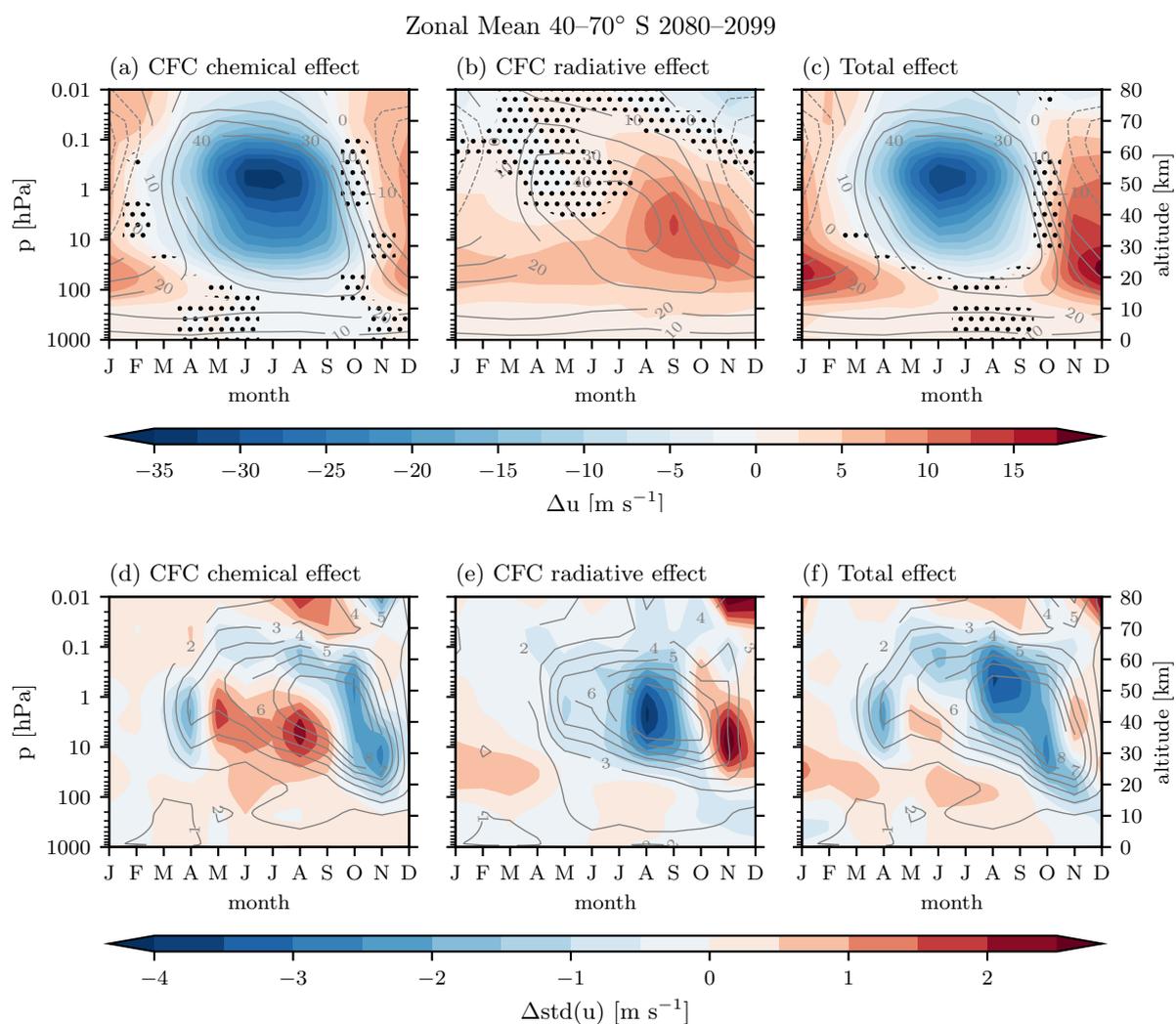

Figure 5. 40-70° S zonal mean wind differences (upper row) and zonal mean standard deviation differences for zonal wind (bottom row) for each month of 2080-2099. The left column shows CFC chemical effect (noMPA_CFCRadOFF–ref), the center column the CFC radiative effect (noMPA–noMPA_CFCRadOFF) and the right column the total effect of CFC chemical and CFC radiative effect combined (noMPA– ref). Stippling indicates not significant at a 90 % confidence level. The contour lines indicate the ref zonal wind profile in the top row and the ref standard deviation in the bottom row. Note that the color saturation is different for negative and positive values.
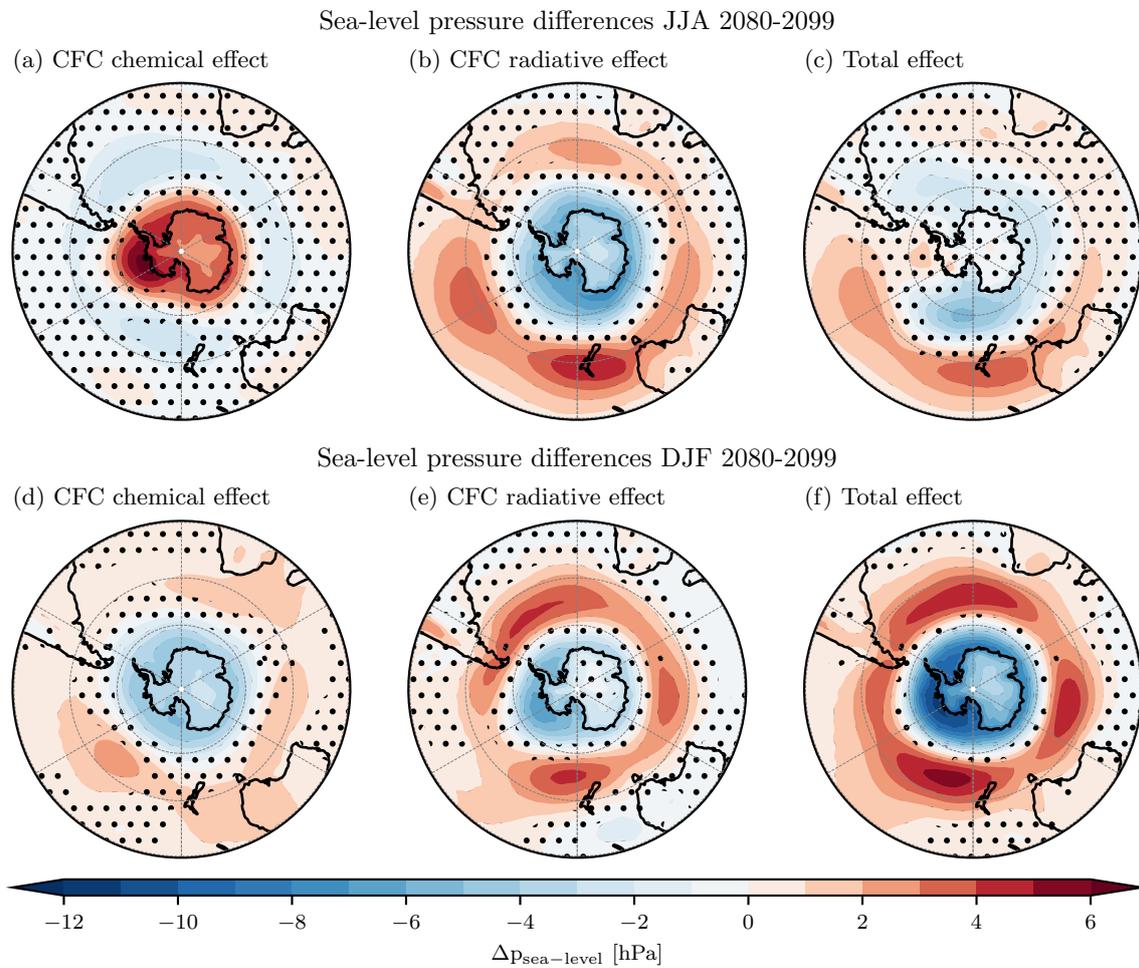
Sea-level pressure differences JJA 2080-2099

(a) CFC chemical effect (b) CFC radiative effect (c) Total effect

Sea-level pressure differences DJF 2080-2099

(d) CFC chemical effect (e) CFC radiative effect (f) Total effect

$\Delta p_{sea-level}$ [hPa]

Figure 6. 2080-2099 Antarctic winter (upper row) and summer (lower row) sea-level pressure differences. CFC chemical effect (a, d), CFC radiative effect (b, e) and total effect (c, f). Stippling indicates not significant at a 90 % confidence level.

3.4 NAO response

Sea-level pressure differences DJF 2080-2099

(a) CFC chemical effect   (b) CFC radiative effect   (c) Total effect

$\Delta\mathrm{p_{sea-level}}$ [hPa]
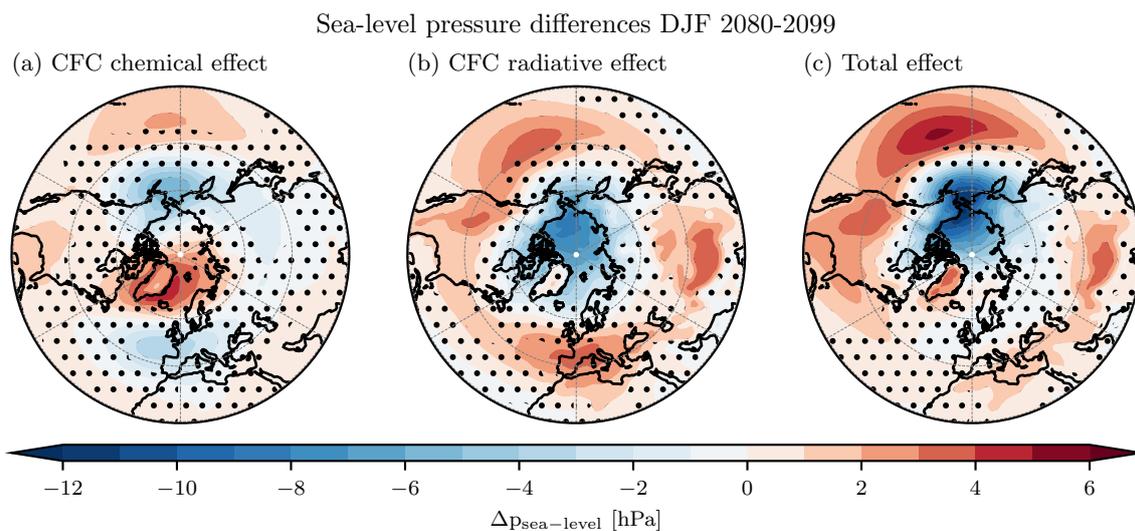
Figure 7. 2080-2099 Arctic winter sea-level pressure differences. CFC chemical effect (a), CFC radiative effect (b) and total effect (c). Stippling indicates not significant at a 90 % confidence level.

The previous results show that the absence of the MPA and subsequent changes in ozone lead to drastic changes in the stratospheric circulation and also influence the tropospheric circulation in the SH. Similar to the SH, large-scale climate variability in Europe and the North Atlantic can be described by the North Atlantic Oscillation (NAO) (Fig. 7. for winter, F3 for the other seasons). The weakening of the polar vortex in the NH due to the CFC chemical effect, i.e. ozone depletion, is reflected in the decrease of the meridional near surface pressure gradient in Fig. 7a. The NH shows an increase of pressure in winter in the polar regions and a decrease in mid-latitudes, shifting the NAO to a more negative phases. The NAO− pattern is also strongly reflected in the surface temperature response in Fig. 8b (DJF and MAM), with a warming over eastern Canada and a severe cooling over northern Eurasia. For the radiative CFC effect, the NAO shows the opposite signal year round with varying strength. It shifts to a more positive phase, i.e the near surface pressure gradient between the mid and high latitudes increases (Figures 7b, for the other seasons F1 middle column). It is most likely that this response does not originate from the stratosphere, as stratospheric changes induced by CFCs are small (see Fig. 3b and e), but arises from the CFCs induced warming in the troposphere and in particular, the upper tropical troposphere. Their GHG effect is similar to what is observed in a changing climate, e.g. Ivanciu et al. (2022). The combined CFC effects cancel each other out in winter in the NH Atlantic region (Fig. 7c), i.e. the NAO is unaffected by the collapse of the ozone layer.

13
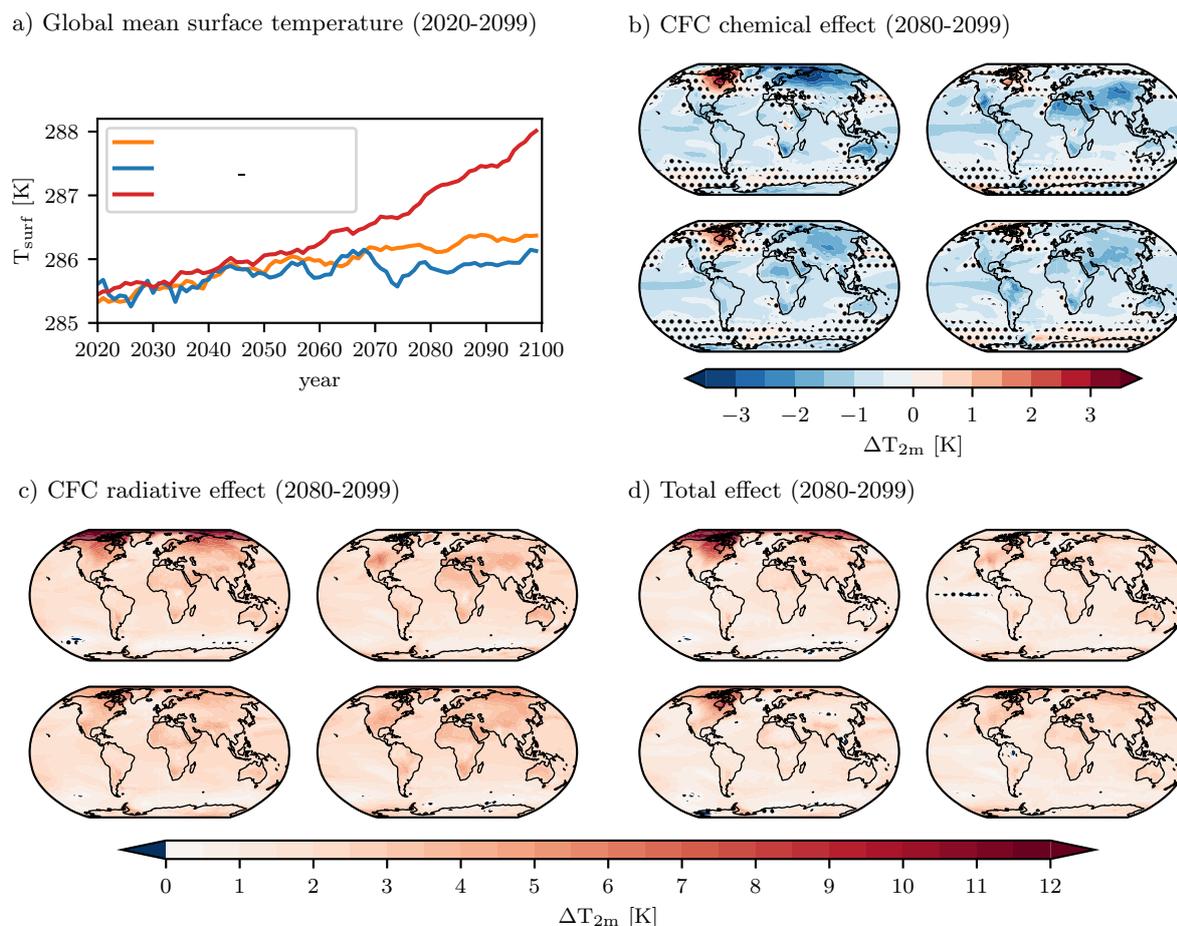
3.5 Surface temperature response

Figure 8. Surface temperatures: a) Global mean surface temperature evolution for the two No-MPA scenarios and the reference from 2020-2099, (b)–(d) global surface temperature for the CFC chemical effect, the CFC radiative effect and the total effect at the end of the century. Stippling indicates not significant at a 90 % confidence level.

As a consequence of the abundance of CFCs and their large greenhouse gas potential, the global surface temperature rises in the noMPA experiment by almost 3.5 K compared to 1980 and is around 1.9 K higher than the reference experiment at the end of the century (red line in Fig. 8a). This is similar to the warming at the end of the century obtained with the SSP5-8.5 scenario at the end of the century (Egorova et al., 2022). When the CFC warming is not considered (noMPA_CFCRadOff), the ozone depletion leads to a decrease in surface temperature at the end of the century (blue line in Fig. 8a) by 0.6 K compared to the reference (orange line in Fig. 8a). This temperature decrease is also depicted in Fig. 8b. For the boreal winter, we obtain the strongest cooling exceeding −3 K over northern Eurasia, whereas northern Canada experiences a warming of up to 3 K. This warming is most likely part of the dynamical response and the resulting negative NAO phase, due to the weakening of the

240

245 stratospheric polar vortex discussed above. These regional temperature changes are due to e.g. reduced advection of mild air over Eurasia (e.g. Hurrell J.W., 1995; Visbeck et al., 2001). The CFC radiative effect increases surface temperature by around 2.5 K globally, with the strongest signal of an over 12 K increase in the northern polar regions in DJF (Fig. 8c), which leads to a net warming of 1.9 K globally (Fig. 8d). The most pronounced effect is seen over northern Canada where the warming from the ozone depletion adds to the CFC radiative effect, leading to an overall warming of over 13 K. As seen from the temperature

250 evolution in Fig. 8a, the CFC warming effect starts to overpower the cooling from ozone at around 2055. Taken together, we find that the avoided warming due to the MPA is largely modulated - at the regional scale - by the large-scale circulation changes induced by ozone and alterations in stratosphere-troposphere coupling. In addition, we find that globally, only a minor fraction (30 %) of the surface heating due to CFCs (via long wave trapping) is offset by the cooling due to the resulting ozone depletion, consistent with recent work examining the radiative forcing (Chiodo and Polvani, 2022).

255 4 Conclusions

We conducted a set of experiments with the ESM SOCOLv4, where we investigated changes in large-scale circulation of the stratosphere and troposphere under the extreme conditions of a No-Montreal-Protocol scenario at the end of the 21st century.

The key novelty over previous studies lies in our detailed separation of the effects induced by abundant CFCs: the chemical (i.e. ozone depletion) and radiative (i.e. global warming) properties of CFCs. To achieve this, we carried out experiments

260 where CFCs were active and inactive for the radiation scheme. The main results of the CFC chemical effect are summarized as follows:

   – Unabated CFC emissions deplete up to 90 % of ozone in the stratosphere at the end of the 21st century, severely decreasing shortwave heating there and leading to a cooling of the global stratosphere by up to 30 K.

   – The cooling is particularly pronounced in the tropical stratosphere, reducing the equator-to-pole temperature gradient in

265 both hemispheres, and consequently also largely weakening the winter polar vortices in both hemispheres.

   – The weaker wintertime vortices shift the tropospheric SAM to a more negative phase in winter and spring as well as the NAO (winter only). Additionally, the SH wintertime polar vortex variability decreases.

   – In austral summer and beginning of fall, westerly winds in the SH stratosphere strengthen causing a shift to a more positive SAM in the troposphere, and a decrease in the wind variability.

270 – The global surface temperature decreases by 0.6 K with a regional warming of 3 K over northern Canada and cooling of −3 K over northern Eurasia. These regional patterns are largely modulated by the changes in the large-scale tropospheric circulation.

The CFC radiative effect counteracts the chemical effect of CFC-induced ozone depletion Through their longwave absorptivity, CFCs strongly warm the troposphere (by up to 5 K) and the lower stratosphere. Further effects include:

275   – The tropical region is mostly affected by the CFC induced tropospheric warming, which slightly increases the equator-to-pole gradient, leading to slightly stronger wintertime vortices compared to the CFC chemical effect.

    – The slightly stronger vortex, and thus decreased variability, together with the strong tropospheric warming of CFCs, shifts the tropospheric SAM to a more positive phase year round and the NAO in winter only.

    – The global surface temperature increases by 2.5 K with the strongest warming by up to 12 K over the Arctic regions.

280 Taken together, the CFC chemical effects largely shaped the stratospheric temperature and circulation changes, whereas the CFC radiative effects are the dominant drivers of the tropospheric large scale circulation and surface temperature changes. In the troposphere, the radiative effects of CFCs overcompensate the changes resulting from ozone depletion (i.e. the CFC chemical effect). The combined CFC chemical and radiative effect are:

    – The BDC speeds up, but with clearly distinct roles of chemical and radiative effects. The shallow branch is mostly
285   affected by the CFC chemical effect and the air becomes over a year younger, whereas the deep branch is mainly influenced by the CFC warming.

    – Both effects cancel each other out for NAO leaving it nearly unchanged under No-MPA conditions.

    – The tropospheric SAM is more positive for austral summer and fall, when CFC chemical and radiative effect reinforce their positive phases consistent with previous work on the ozone hole and its impacts on summertime circulation trends
290   in the SH (World Meteorological Organization (WMO), 2018) and weaker SAM+ signals for winter and spring when both effects are in antiphase.

    – The global surface temperature increases by 1.9 K with the Arctic region being mostly affected in boreal winter and spring, whereas the Antarctic region is fairly buffered and follows the mean global increase.

Overall, the MPA has prevented not only severe implications for our health, but also avoided substantial changes in our sur-
295 face climate. Besides the well known global warming effect of CFCs with subsequent tropospheric circulation changes, we showed that the dynamical changes in the stratosphere, caused by severe ozone depletion, would have also strongly affected the tropospheric variability modes, resulting in regional amplification of adverse effects on surface climate.
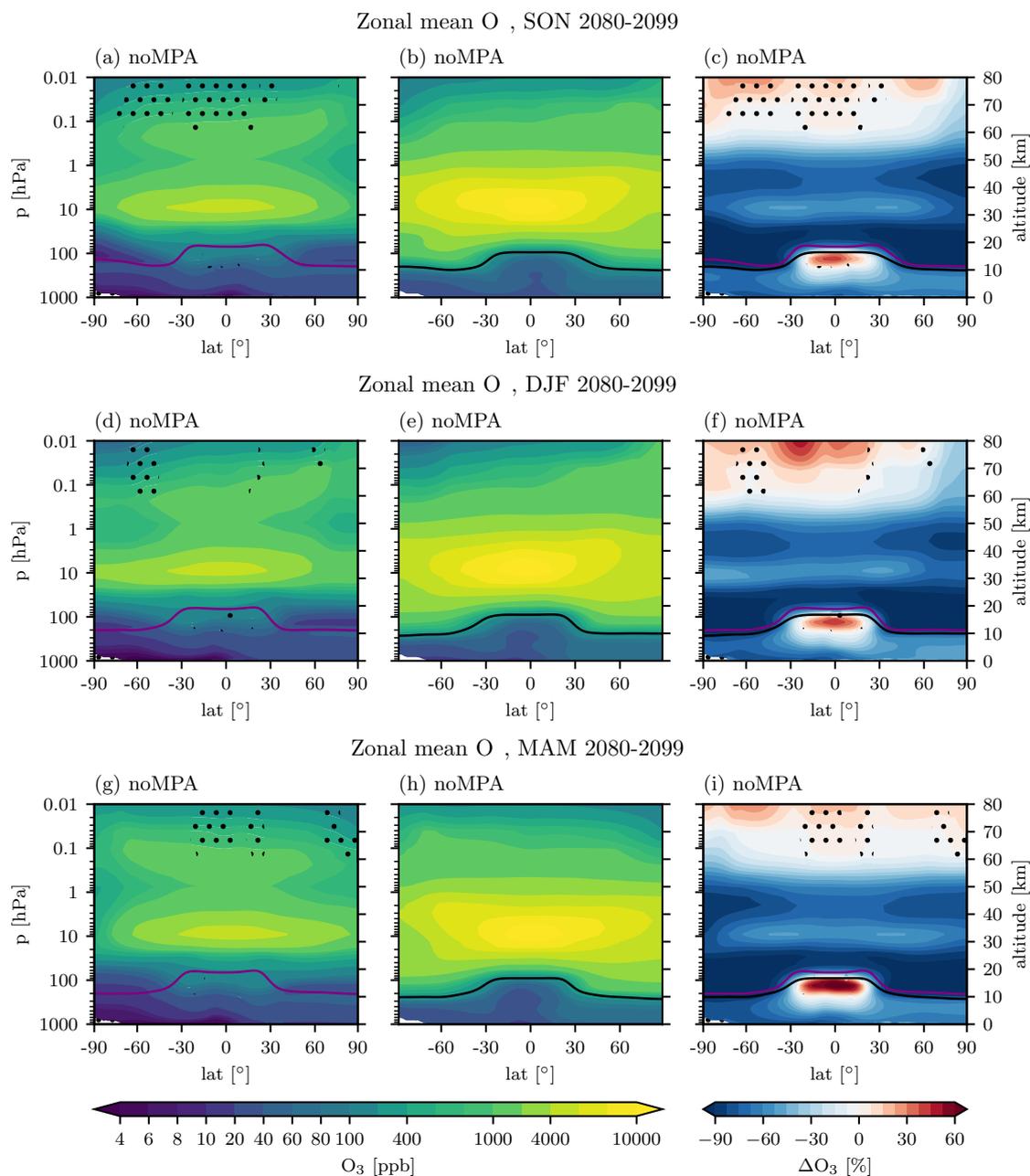
Appendix A: Ozone

Figure A1. 2080–2099 zonal mean ozone noMPA (a), ref (b) and differences in % of noMPA-ref (c) for SON (top), DJF (middle) and MAM (bottom) 2080-2099. The tropopause height is indicated in purple for the noMPA and in black for the MPA reference experiment. Stippling indicates not significant at a 90 % confidence level. Colorbar levels are evenly numbered in log spacing.
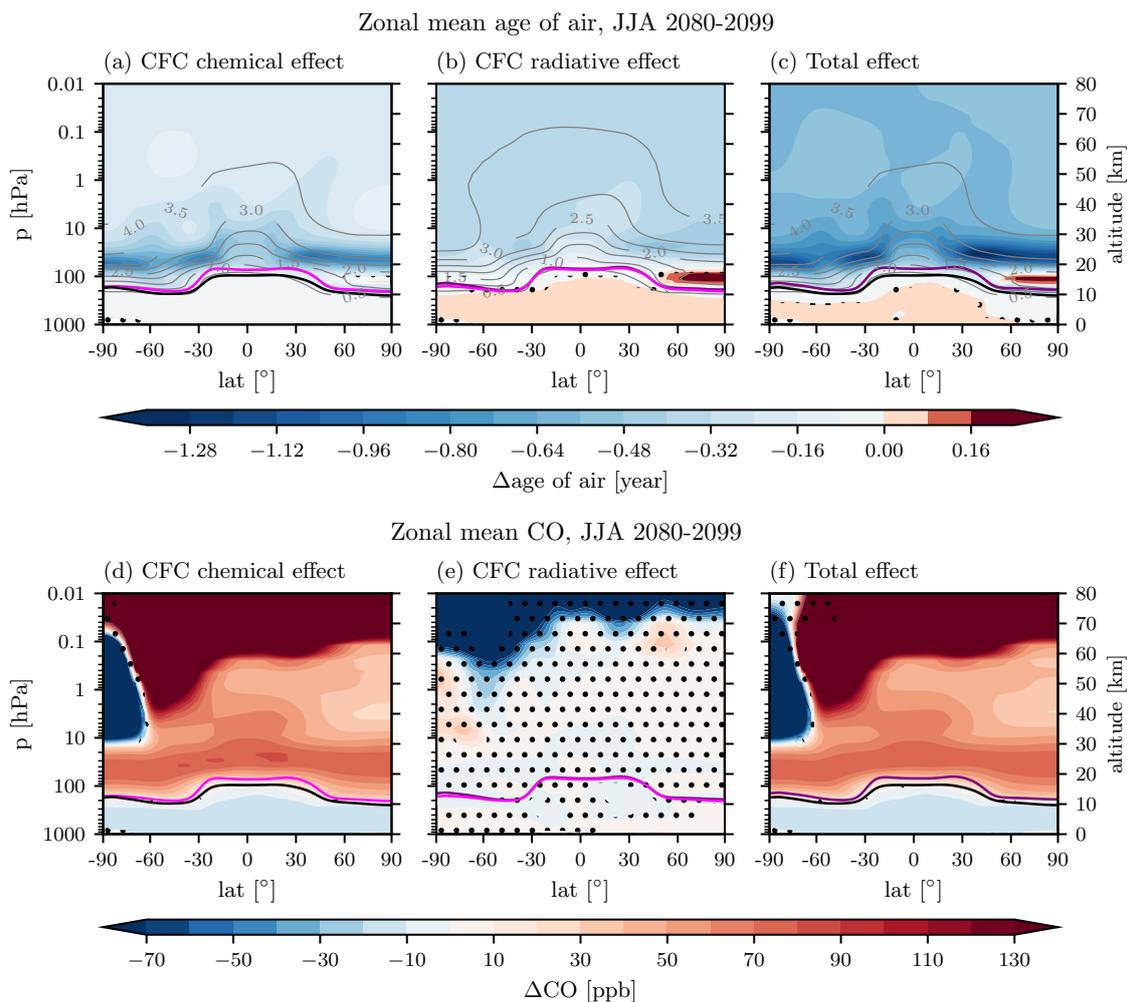
Appendix B: Brewer-Dobson circulation

Figure B1. Top: age of air for JJA (other seasons look very similar) 2080-2099, bottom: CO. The left column shows the CFC chemical effect, the center column the CFC radiative effect and the right column the total effect of CFC chemical and radiative effect combined. Stippling indicates not significant at a 90 % confidence level. The tropopause height is indicated in purple for the noMPA, in magenta for noMPA_CFCRadOff and in black for the reference experiment.

Appendix C: Temperature
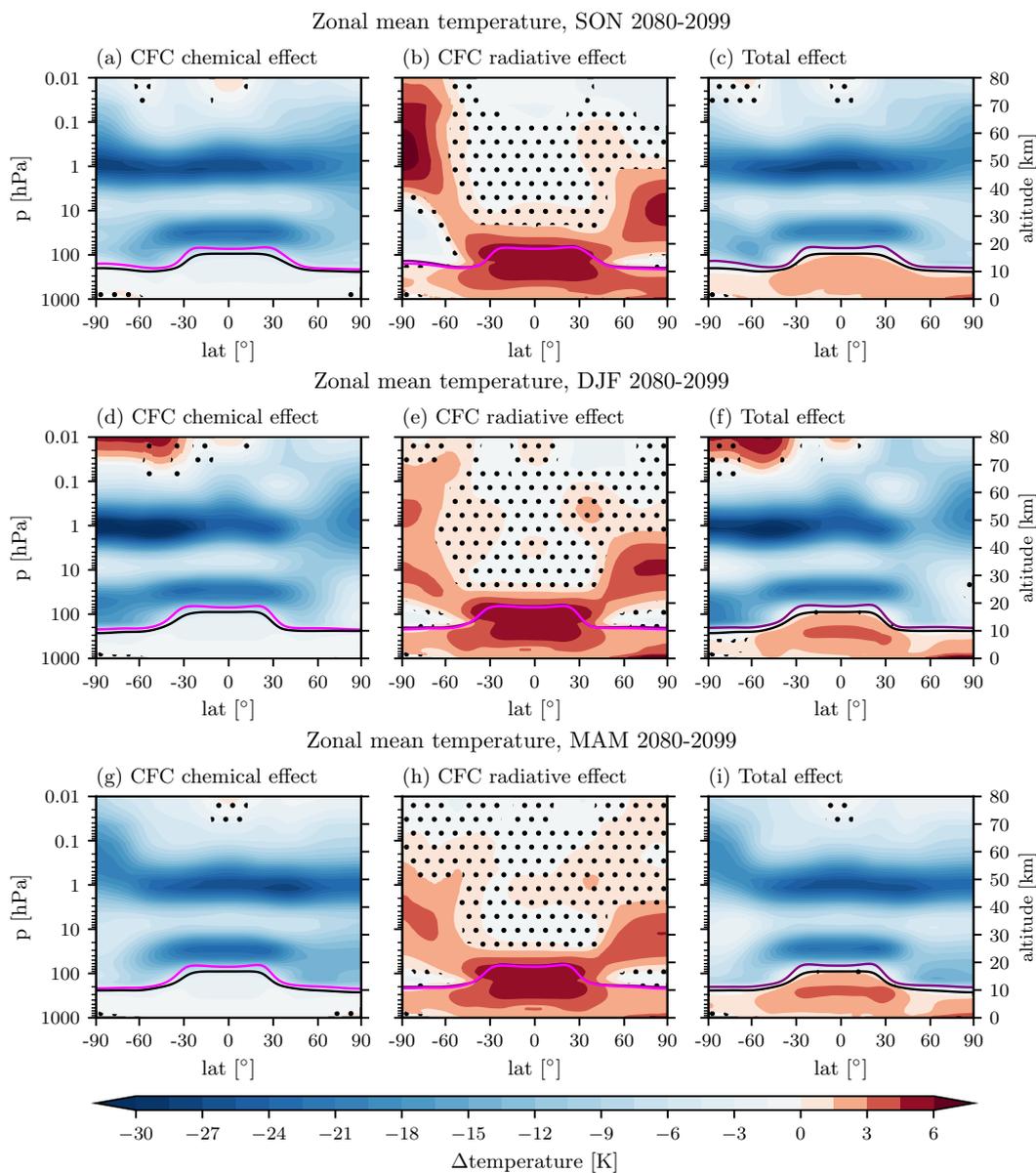
Figure C1. 2080–2099 zonal mean temperature differences in % SON (upper row), DJF (middle row) and MAM (bottom row). The left column shows the CFC chemical effect, the center column the CFC radiative effect and the right column the total effect of CFC chemical and radiative effect combined. Stippling indicates not significant at a 90 % confidence level. The tropopause height is indicated in purple for the noMPA, in magenta for noMPA_CFCRadOff and in black for the reference experiment. Note that the color saturation for temperature is different for negative and positive values.

305 Appendix D: Temperature profile
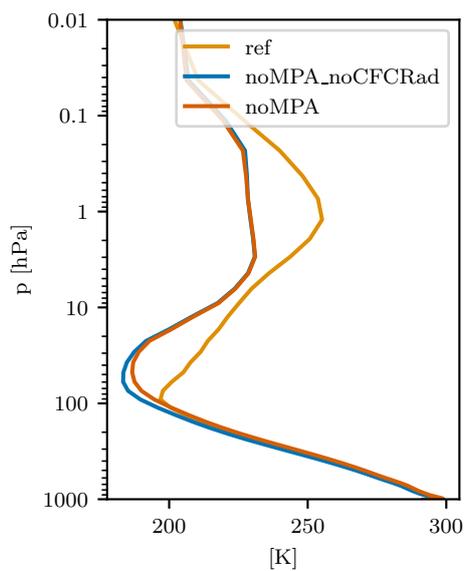
Figure D1. Tropical (30° N–S) zonal mean temperature profiles of noMPA, noMPA_CFCRadOff and ref in JJA 2080-2099.
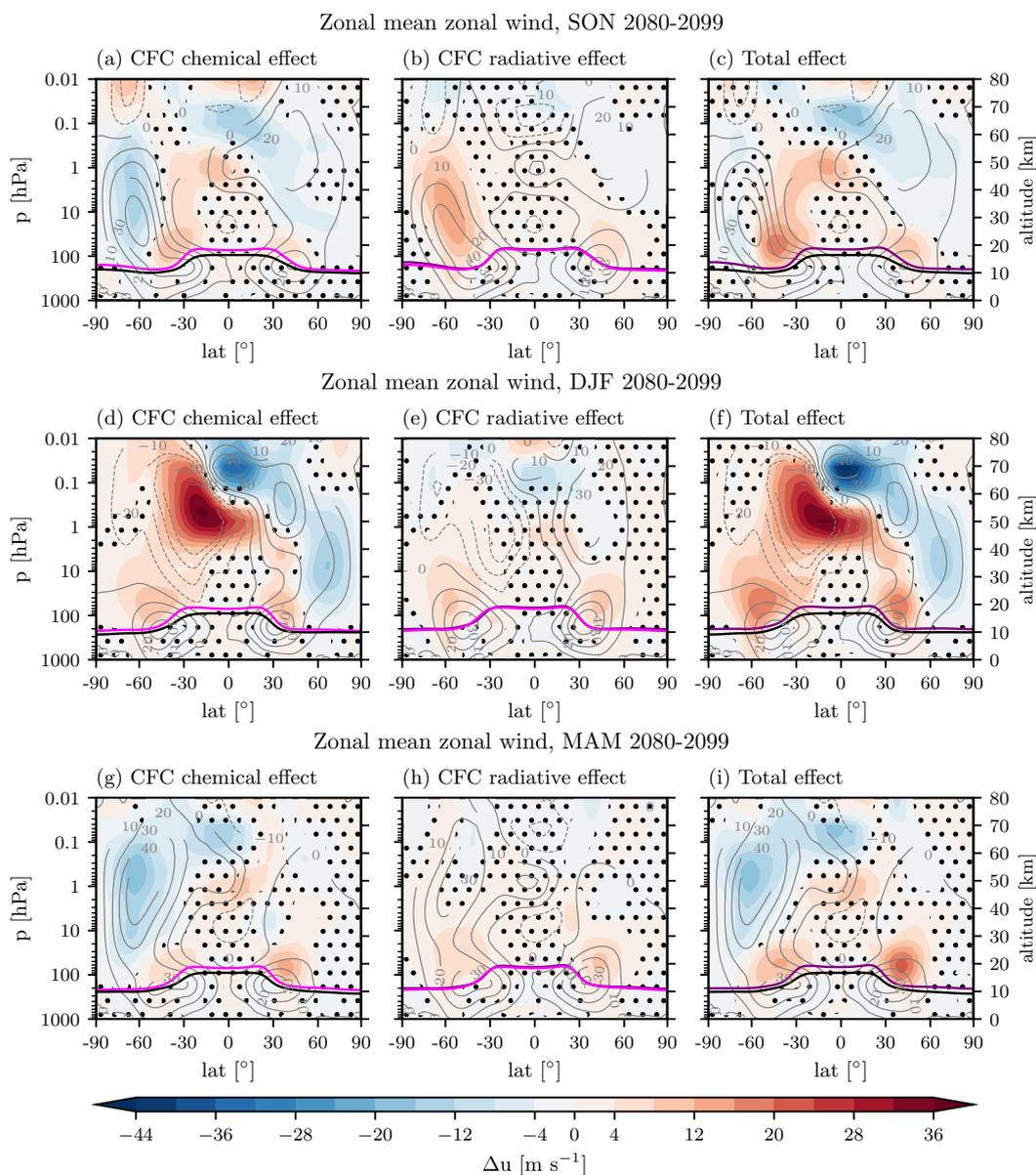
Appendix E: Zonal wind

Figure E1. 2080–2099 zonal mean zonal wind differences in % SON (upper row), DJF (middle row) and MAM (bottom row). The left column shows the CFC chemical effect, the center column the CFC radiative effect and the right column the total effect of CFC chamical and radiative effect combined. Stippling indicates not significant at a 90 % confidence level. The tropopause height is indicated in purple for the noMPA, in magenta for noMPA_CFCRadOff and in black for the reference experiment. The contour lines indicate the ref zonal wind profile.

Appendix F: Surface

Sea-level pressure differences SON 2080-2099

(a) CFC chemical effect   (b) CFC radiative effect   (c) Total effect

Sea-level pressure differences MAM 2080-2099

(d) CFC chemical effect   (e) CFC radiative effect   (f) Total effect
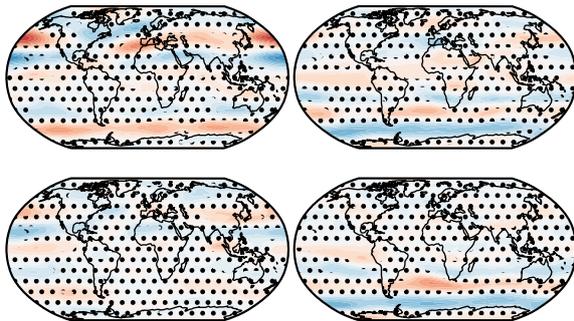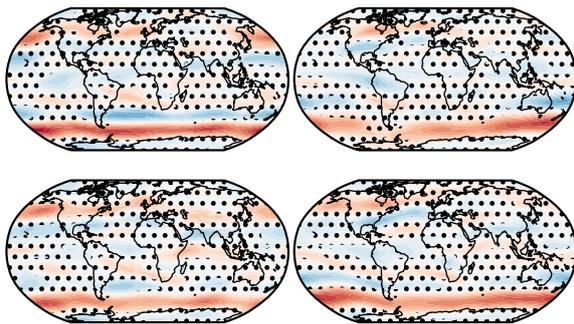

$$\Delta p_{sea-level} \ [hPa]$$
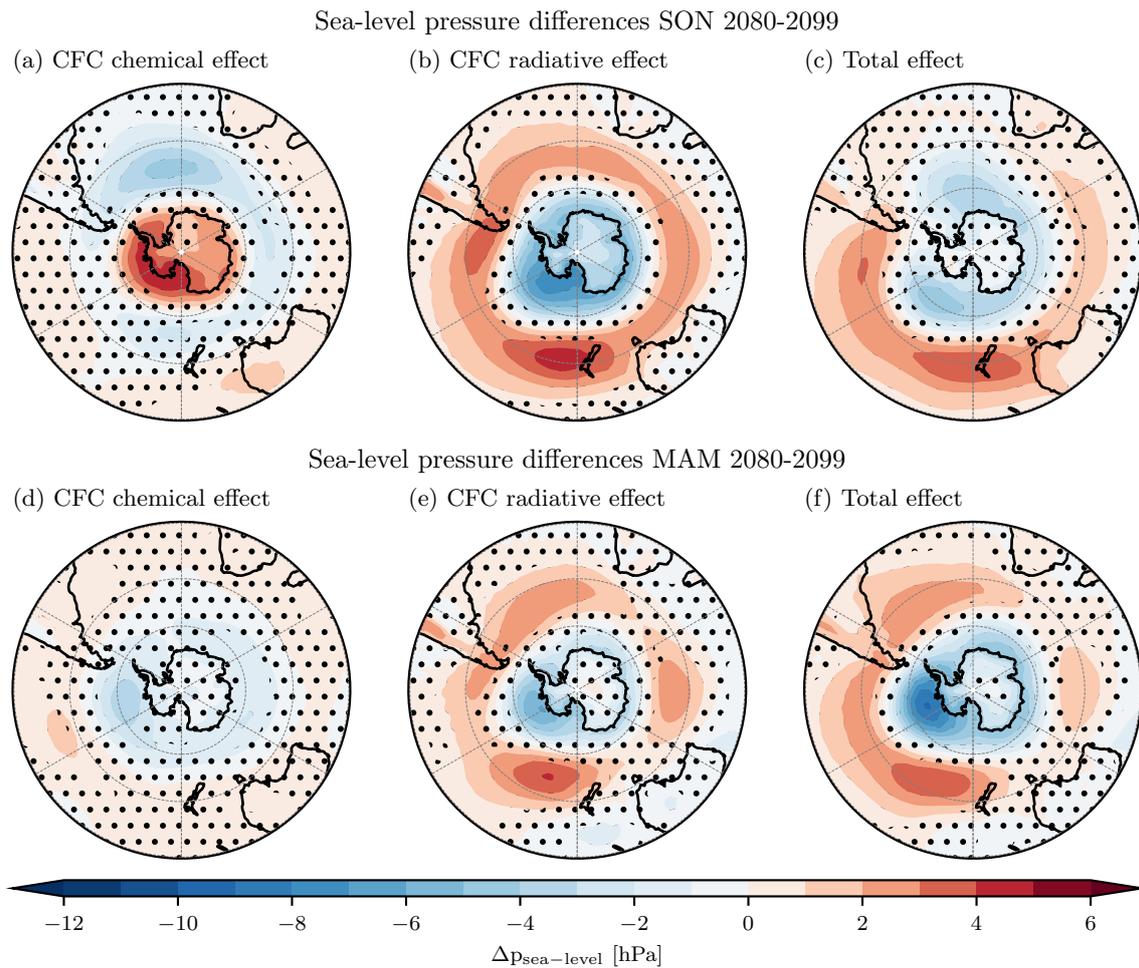
Figure F1. 2080-2099 Antarctic spring and fall sea-level pressure differences. CFC chemical effect (a, d), CFC radiative effect (b, e) and total effect (c, f). Stippling indicates not significant at a 90 % confidence level.

a) CFC chemical effect

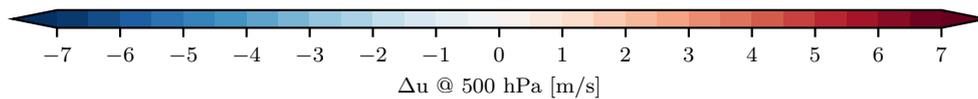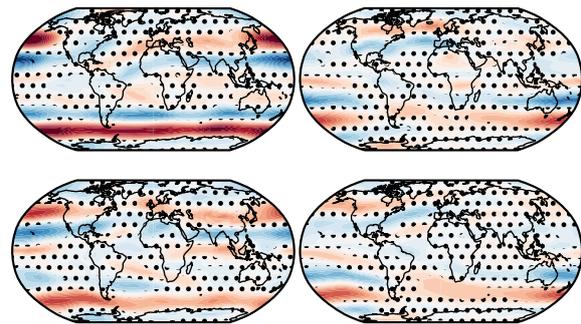b) CFC radiative effect

c) Total effect

Δu @ 500 hPa [m/s]

Figure F2. 2080-2099 zonal wind differences at 500 hPa. CFC chemical effect (a), CFC radiative effect (b) and total effect (c). Stippling indicates not significant at a 90 % confidence level.
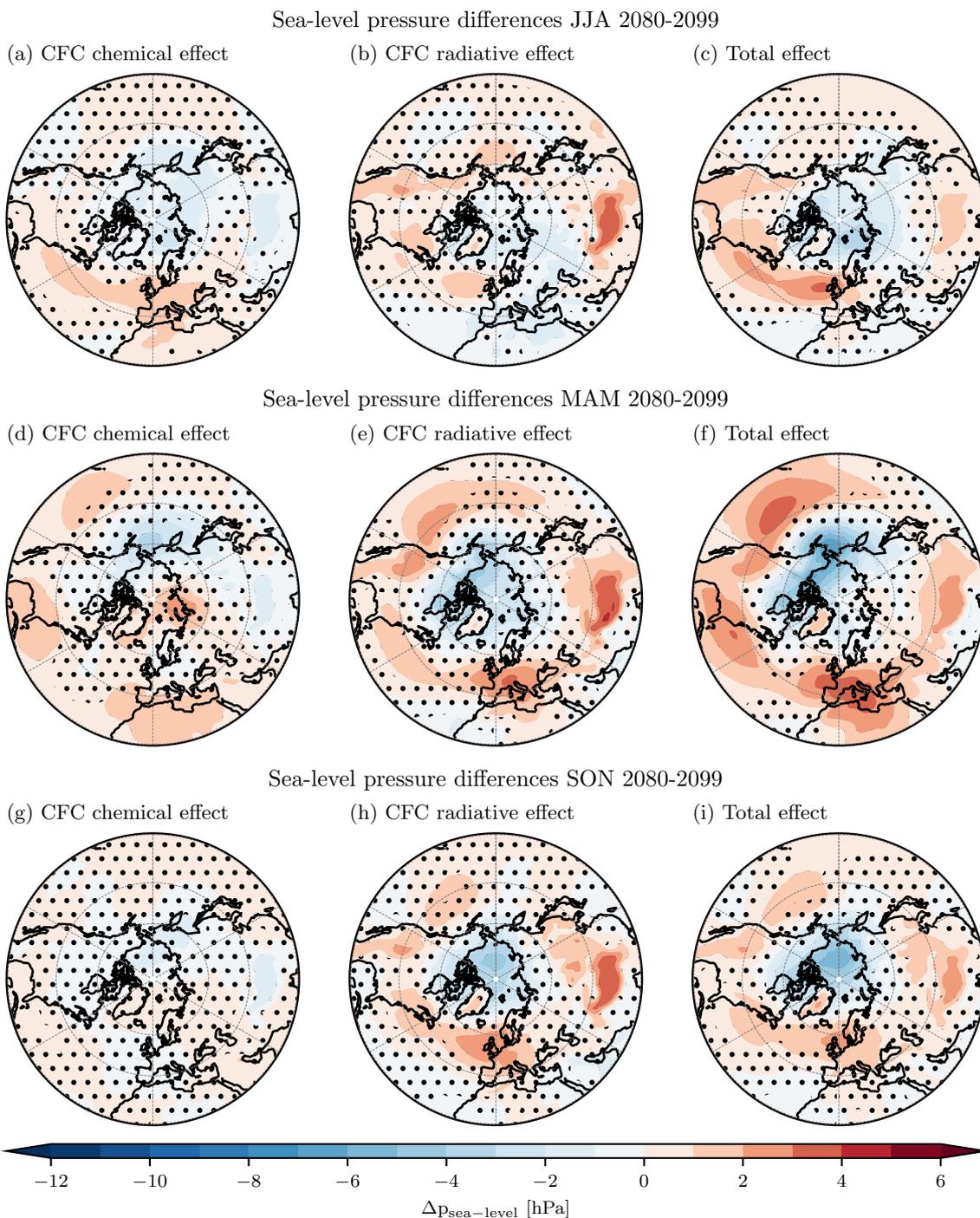
Figure F3. 2080-2099 Arctic spring, summer and fall sea-level pressure differences. CFC chemical effect (a, d, g), CFC radiative effect (b, e, h) and total effect (c, f, i). Stippling indicates not significant at a 90 % confidence level.

Competing interests. The authors declare that they have no conflict of interest.

References

Abalos, M., Polvani, L., Calvo, N., Kinnison, D., Ploeger, F., Randel, W., and Solomon, S.: New Insights on the Impact of Ozone-Depleting Substances on the Brewer-Dobson Circulation, Journal of Geophysical Research: Atmospheres, 124, 2435–2451, https://doi.org/10.1029/2018JD029301, 2019.

320

Ball, W. T., Kuchai, A., Rozanov, E. V., Staehelin, J., Tummon, F., Smith, A. K., Sukhodolov, T., Stenke, A., Revell, L., Coulon, A., Schmutz, W., and Peter, T.: An upper-branch Brewer-Dobson circulation index for attribution of stratospheric variability and improved ozone and temperature trend analysis, Atmospheric Chemistry and Physics, 16, 15 485–15 500, https://doi.org/10.5194/acp-16-15485-2016, 2016.

Banerjee, A., C. Maycock, A., T. Archibald, A., Luke Abraham, N., Telford, P., Braesicke, P., and A. Pyle, J.: Drivers of changes

325

in stratospheric and tropospheric ozone between year 2000 and 2100, Atmospheric Chemistry and Physics, 16, 2727–2746, https://doi.org/10.5194/acp-16-2727-2016, 2016.

Banerjee, A., Fyfe, J. C., Polvani, L. M., Waugh, D., and Chang, K. L.: A pause in Southern Hemisphere circulation trends due to the Montreal Protocol, Nature, 579, 544–548, https://doi.org/10.1038/s41586-020-2120-4, 2020.

Barnes, P. W., Williamson, C. E., Lucas, R. M., Robinson, S. A., Madronich, S., Paul, N. D., Bornman, J. F., Bais, A. F., Sulzberger, B.,

330

Wilson, S. R., Andrady, A. L., McKenzie, R. L., Neale, P. J., Austin, A. T., Bernhard, G. H., Solomon, K. R., Neale, R. E., Young, P. J., Norval, M., Rhodes, L. E., Hylander, S., Rose, K. C., Longstreth, J., Aucamp, P. J., Ballaré, C. L., Cory, R. M., Flint, S. D., de Gruijl, F. R., Häder, D. P., Heikkilä, A. M., Jansen, M. A., Pandey, K. K., Robson, T. M., Sinclair, C. A., Wängberg, S. Å., Worrest, R. C., Yazar, S., Young, A. R., and Zepp, R. G.: Ozone depletion, ultraviolet radiation, climate change and prospects for a sustainable future, Nature Sustainability, 2, 569–579, https://doi.org/10.1038/s41893-019-0314-2, 2019.

335

Calvo, N., Polvani, L. M., and Solomon, S.: On the surface impact of Arctic stratospheric ozone extremes, Environmental Research Letters, 10, https://doi.org/10.1088/1748-9326/10/9/094003, 2015.

Calvo, N., Garcia, R. R., and Kinnison, D. E.: Revisiting Southern Hemisphere polar stratospheric temperature trends in WACCM: The role of dynamical forcing, Geophysical Research Letters, 44, 3402–3410, https://doi.org/10.1002/2017GL072792, 2017.

Chiodo, G. and Polvani, L. M.: The response of the ozone layer to quadrupled CO2 concentrations: Implications for climate, Journal of

340

Climate, 32, 7629–7642, https://doi.org/10.1175/JCLI-D-19-0086.1, 2019.

Chiodo, G. and Polvani, L. M.: New Insights on the Radiative Impacts of Ozone-Depleting Substances, Geophysical Research Letters, 49, 1–11, https://doi.org/10.1029/2021GL096783, 2022.

Chipperfield, M. P. and Pyle, J. A.: Two-Dimensional Modelling of the Antarctic Lower Stratosphere, GEOPHYSICAL RESEARCH LETTER, 15, 875–878, 1988.

345

Dennison, F. W., McDonald, A. J., and Morgenstern, O.: The effect of ozone depletion on the southern annular mode and stratosphere-troposphere coupling, Journal of Geophysical Research, 120, 6305–6312, https://doi.org/10.1002/2014JD023009, 2015.

Domeisen, D. I. and Butler, A. H.: Stratospheric drivers of extreme events at the Earth's surface, Communications Earth and Environment, 1, 1–8, https://doi.org/10.1038/s43247-020-00060-z, 2020.

Egorova, T., Rozanov, E., Gröbner, J., Hauser, M., and Schmutz, W.: Montreal protocol benefits simulated with CCM SOCOL, Atmospheric

350

Chemistry and Physics, 13, 3811–3823, https://doi.org/10.5194/acp-13-3811-2013, 2013.

Egorova, T., Sedlacek, J., Sukhodolov, T., Karagodin-Doyennel, A., Zilker, F., and Rozanov, E.: Montreal Protocol's impact on the ozone layer and climate, Atmospheric Chemistry and Physics Discussions, 2022, 1–19, https://doi.org/10.5194/acp-2022-730, 2022.

Egorova, T. A., Rozanov, E. V., Zubov, V. A., and Karol, I. L.: Model for investigating ozone trends (MEZON), Izvestiya Atmospheric and Oceanic Physics, 39, 277–292, 2003.

355 Feinberg, A., Sukhodolov, T., Luo, B. P., Rozanov, E., Winkel, L. H., Peter, T., and Stenke, A.: Improved tropospheric and strato-spheric sulfur cycle in the aerosol-chemistry-climate model SOCOL-AERv2, Geoscientific Model Development, 12, 3863–3887, https://doi.org/10.5194/gmd-12-3863-2019, 2019.

Friedel, M., Chiodo, G., Stenke, A., Domeisen, D. I., Fueglistaler, S., Anet, J. G., and Peter, T.: Springtime arctic ozone depletion forces northern hemisphere climate anomalies, Nature Geoscience, 15, 541–547, https://doi.org/10.1038/s41561-022-00974-7, 2022.

360 Garcia, R. R., Kinnison, D. E., and Marsh, D. R.: World avoided simulations with the Whole Atmosphere Community Climate Model, Journal of Geophysical Research Atmospheres, 117, 1–16, https://doi.org/10.1029/2012JD018430, 2012.

Gillett, N. P. and Thompson, D. W.: Simulation of recent Southern Hemisphere climate change, Science, 302, 273–275, https://doi.org/10.1126/science.1087440, 2003.

Goyal, R., England, M. H., Sen Gupta, A., and Jucker, M.: Reduction in surface climate change achieved by the 1987 Montreal Protocol,
365 Environmental Research Letters, 14, https://doi.org/10.1088/1748-9326/ab4874, 2019.

Gutiérrez, J., Jones, R., Narisma, G., Alves, L., Amjad, M., Gorodetskaya, I., Grose, M., Klutse, N., Krakovska, S., Li, J., Martínez-Castro, D., Mearns, L., Mernild, S., Ngo-Duc, T., van den Hurk, B., and Yoon, J.-H.: Atlas, in: The Physical Science Basis. Contribution of Working Group I to the Sixth Assessment Report of the Intergovernmental Panel on Climate Change, edited by Masson-Delmotte, V., Zhai, P., Pirani, A., Connors, S., Péan, C., Berger, S., Caud, N., Chen, Y., Goldfarb, L., Gomis, M., Huang, M., Leitzell, K., Lonnoy, E.,
370 Matthews, J., Maycock, T., Waterfield, T., Yelekçi, O., Yu, R., and Zhou, B. e., pp. 1927–2058, Cambridge University Press, Cambridge, United Kingdom and New York, NY, USA, https://doi.org/10.1017/9781009157896.021, 2021.

Hurrell J.W.: Decadal Trends in the North Atlantic Oscillation: Regional Temperatures and Precipitation, Science, 269, 676–679, 1995.

Ivanciu, I., Matthes, K., Biastoch, A., Wahl, S., and Harlaß, J.: Twenty-first-century Southern Hemisphere impacts of ozone recovery and climate change from the stratosphere to the ocean, Weather and Climate Dynamics, 3, 139–171, https://doi.org/10.5194/wcd-3-139-2022,
375 2022.

Ivy, D. J., Solomon, S., Calvo, N., and Thompson, D. W.: Observed connections of Arctic stratospheric ozone extremes to Northern Hemisphere surface climate, Environmental Research Letters, 12, https://doi.org/10.1088/1748-9326/aa57a4, 2017.

Karpechko, A., Maycock, A., authors), L., Abalos, M., Akiyoshi, H., Arblaster, J., Garfinkel, C., Rosenhof, K., and Sigmond, M.: Stratospheric Ozone Changes and Climate, in: Scientific Assessment of Ozone Depletion: 2018, edited by Cagnazzo, C. and Polvani,
380 L., chap. Chapter 5, World Meteorological Organization, Geneva, Switzerland, https://www.esrl.noaa.gov/csd/assessments/ozone/2018/report/Chapter5{_}2018OzoneAssessment.pdf, 2018.

Kidston, J., Scaife, A. A., Hardiman, S. C., Mitchell, D. M., Butchart, N., Baldwin, M. P., and Gray, L. J.: Stratospheric influence on tropospheric jet streams, storm tracks and surface weather, Nature Geoscience, 8, 433–440, https://doi.org/10.1038/NGEO2424, 2015.

Mauritsen, T., Bader, J., Becker, T., Behrens, J., Bittner, M., Brokopf, R., Brovkin, V., Claussen, M., Crueger, T., Esch, M., Fast, I., Fiedler,
385 S., Fläschner, D., Gayler, V., Giorgetta, M., Goll, D. S., Haak, H., Hagemann, S., Hedemann, C., Hohenegger, C., Ilyina, T., Jahns, T., Jimenéz-de-la Cuesta, D., Jungclaus, J., Kleinen, T., Kloster, S., Kracher, D., Kinne, S., Kleberg, D., Lasslop, G., Kornblueh, L., Marotzke, J., Matei, D., Meraner, K., Mikolajewicz, U., Modali, K., Möbis, B., Müller, W. A., Nabel, J. E. M. S., Nam, C. C. W., Notz, D., Nyawira, S.-S., Paulsen, H., Peters, K., Pincus, R., Pohlmann, H., Pongratz, J., Popp, M., Raddatz, T. J., Rast, S., Redler, R., Reick, C. H., Rohrschneider, T., Schemann, V., Schmidt, H., Schnur, R., Schulzweida, U., Six, K. D., Stein, L., Stemmler, I., Stevens, B., von
390 Storch, J.-S., Tian, F., Voigt, A., Vrese, P., Wieners, K.-H., Wilkenskjeld, S., Winkler, A., and Roeckner, E.: Developments in the MPI-M

Earth System Model version 1.2 (MPI-ESM1.2) and Its Response to Increasing CO2, Journal of Advances in Modeling Earth Systems, 11, 998–1038, https://doi.org/https://doi.org/10.1029/2018MS001400, 2019.

Meng, L., Liu, J., Tarasick, D. W., Randel, W. J., Steiner, A. K., Wilhelmsen, H., Wang, L., and Haimberger, L.: Continuous rise of the tropopause in the Northern Hemisphere over 1980-2020, Science Advances, 7, 1–10, https://doi.org/10.1126/sciadv.abi8065, 2021.

395 Morgenstern, O., Braesicke, P., Hurwitz, M. M., O'Connor, F. M., Bushell, A. C., Johnson, C. E., and Pyle, J. A.: The world avoided by the Montreal Protocol, Geophysical Research Letters, 35, 1–5, https://doi.org/10.1029/2008GL034590, 2008.

Morgenstern, O., O'Connor, F. M., Johnson, B. T., Zeng, G., Mulcahy, J. P., Williams, J., Teixeira, J., Michou, M., Nabat, P., Horowitz, L. W., Naik, V., Sentman, L. T., Deushi, M., Bauer, S. E., Tsigaridis, K., Shindell, D. T., and Kinnison, D. E.: Reappraisal of the Climate Impacts of Ozone-Depleting Substances, Geophysical Research Letters, 47, https://doi.org/10.1029/2020GL088295, 2020.

400 Morgenstern, O., Frith, S. M., Bodeker, G. E., Fioletov, V., and van der A, R. J.: Reevaluation of Total-Column Ozone Trends and of the Effective Radiative Forcing of Ozone-Depleting Substances, Geophysical Research Letters, 48, https://doi.org/10.1029/2021GL095376, 2021.

Morgenstern, O., Kinnison, D. E., Mills, M., Michou, M., Horowitz, L. W., Lin, P., Deushi, M., Yoshida, K., O'Connor, F. M., Tang, Y., Abraham, N. L., Keeble, J., Dennison, F., Rozanov, E., Egorova, T., Sukhodolov, T., and Zeng, G.: Comparison of Arctic and Antarc-
405 tic Stratospheric Climates in Chemistry Versus No-Chemistry Climate Models, Journal of Geophysical Research: Atmospheres, 127, https://doi.org/10.1029/2022JD037123, 2022.

Neale, R. E., Barnes, P. W., Robson, T. M., Neale, P. J., Williamson, C. E., Zepp, R. G., Wilson, S. R., Madronich, S., Andrady, A. L., Heikkilä, A. M., Bernhard, G. H., Bais, A. F., Aucamp, P. J., Banaszak, A. T., Bornman, J. F., Bruckman, L. S., Byrne, S. N., Foereid, B., Häder, D. P., Hollestein, L. M., Hou, W. C., Hylander, S., Jansen, M. A., Klekociuk, A. R., Liley, J. B., Longstreth, J., Lucas, R. M.,
410 Martinez-Abaigar, J., McNeill, K., Olsen, C. M., Pandey, K. K., Rhodes, L. E., Robinson, S. A., Rose, K. C., Schikowski, T., Solomon, K. R., Sulzberger, B., Ukpebor, J. E., Wang, Q. W., Wängberg, S., White, C. C., Yazar, S., Young, A. R., Young, P. J., Zhu, L., and Zhu, M.: Environmental effects of stratospheric ozone depletion, UV radiation, and interactions with climate change: UNEP Environmental Effects Assessment Panel, Update 2020, vol. 20, Springer International Publishing, https://doi.org/10.1007/s43630-020-00001-x, 2021.

Newman, P. A., Oman, L. D., Douglass, A. R., Fleming, E. L., Frith, S. M., Hurwitz, M. M., Kawa, S. R., Jackman, C. H., Krotkov,
415 N. A., Nash, E. R., Nielsen, J. E., Pawson, S., Stolarski, R. S., and Velders, G. J.: What would have happened to the ozone layer if chlorofluorocarbons (CFCs) had not been regulated?, Atmospheric Chemistry and Physics, 9, 2113–2128, https://doi.org/10.5194/acp-9-2113-2009, 2009.

Polvani, L. M., Wang, L., Abalos, M., Butchart, N., Chipperfield, M. P., Dameris, M., Deushi, M., Dhomse, S. S., Jöckel, P., Kinnison, D., Michou, M., Morgenstern, O., Oman, L. D., Plummer, D. A., and Stone, K. A.: Large Impacts, Past and Future, of Ozone-Depleting
420 Substances on Brewer-Dobson Circulation Trends: A Multimodel Assessment, Journal of Geophysical Research: Atmospheres, 124, 6669–6680, https://doi.org/10.1029/2018JD029516, 2019.

Previdi, M. and Polvani, L. M.: Climate system response to stratospheric ozone depletion and recovery, Quarterly Journal of the Royal Meteorological Society, 140, 2401–2419, https://doi.org/10.1002/qj.2330, 2014.

Randel, W. J., Smith, A. K., Wu, F., Zou, C. Z., and Qian, H.: Stratospheric temperature trends over 1979-2015 derived from combined SSU,
425 MLS, and SABER satellite observations, Journal of Climate, 29, 4843–4859, https://doi.org/10.1175/JCLI-D-15-0629.1, 2016.

Riahi, K., van Vuuren, D. P., Kriegler, E., Edmonds, J., O'Neill, B. C., Fujimori, S., Bauer, N., Calvin, K., Dellink, R., Fricko, O., Lutz, W., Popp, A., Cuaresma, J. C., KC, S., Leimbach, M., Jiang, L., Kram, T., Rao, S., Emmerling, J., Ebi, K., Hasegawa, T., Havlik, P., Humpenöder, F., Da Silva, L. A., Smith, S., Stehfest, E., Bosetti, V., Eom, J., Gernaat, D., Masui, T., Rogelj, J., Strefler, J., Drouet,

430   L., Krey, V., Luderer, G., Harmsen, M., Takahashi, K., Baumstark, L., Doelman, J. C., Kainuma, M., Klimont, Z., Marangoni, G., Lotze-Campen, H., Obersteiner, M., Tabeau, A., and Tavoni, M.: The Shared Socioeconomic Pathways and their energy, land use, and greenhouse gas emissions implications: An overview, Global Environmental Change, 42, 153–168, https://doi.org/10.1016/j.gloenvcha.2016.05.009, 2017.

Santer, B. D., Wehner, M. F., Wigley, T. M. L., Sausen, R., Meehl, G. A., Taylor, K. E., Ammann, C., Arblaster, J., Washington, W. M., Boyle, J. S., and Brüggemann, W.: Contributions of Anthropogenic and Natural Forcing to Recent Tropopause Height Changes, Science, 301, 27–29, 2003.

Shindell, D., Faluvegi, G., Nazarenko, L., Bowman, K., Lamarque, J. F., Voulgarakis, A., Schmidt, G. A., Pechony, O., and Ruedy, R.: Attribution of historical ozone forcing to anthropogenic emissions, Nature Climate Change, 3, 567–570, https://doi.org/10.1038/nclimate1835, 2013.

Shine, K. P.: On the Modelled Thermal Response of the Antarctic Stratosphere to a depletion of ozone, GEOPHYSICAL RESEARCH LETTER, 13, 1331–1334, 1986.

Solomon, S.: Stratospheric ozone depletion: A review of concepts and history, Reviews of Geophysics, 37, 275–316, https://doi.org/10.1029/1999RG900008, 1999.

Sukhodolov, T., Egorova, T., Stenke, A., Ball, W. T., Brodowsky, C., Chiodo, G., Feinberg, A., Friedel, M., Karagodin-Doyennel, A., Peter, T., Sedlacek, J., Vattioni, S., and Rozanov, E.: Atmosphere-ocean-aerosol-chemistry-climate model SOCOLv4.0: Description and evaluation, Geoscientific Model Development, 14, 5525–5560, https://doi.org/10.5194/gmd-14-5525-2021, 2021.

Thompson, D. W. and Solomon, S.: Interpretation of recent Southern Hemisphere climate change, Science, 296, 895–899, https://doi.org/10.1126/science.1069270, 2002.

Thompson, D. W. J., Baldwin, M. P., and Solomon, S.: Stratosphere - Troposphere Coupling in the Southern Hemisphere, Journal of Atmospheric Sciences, 62, 708–715, 2005.

Velders, G. J., Andersen, S. O., Daniel, J. S., Fahey, D. W., and McFarland, M.: The importance of the Montreal Protocol in protecting climate, Proceedings of the National Academy of Sciences of the United States of America, 104, 4814–4819, https://doi.org/10.1073/pnas.0610328104, 2007.

Visbeck, M. H., Hurrell, J. W., Polvani, L., and Cullen, H. M.: The North Atlantic oscillation: Past, present, and future, Proceedings of the National Academy of Sciences of the United States of America, 98, 12 876–12 877, https://doi.org/10.1073/pnas.231391598, 2001.

Weisenstein, D. K., Yue, G. K., Ko, M. K. W., Sze, N.-D., Rodriguez, J. M., and Scott, C. J.: A two-dimensional model of sulfur species and aerosols, Journal of Geophysical Research: Atmospheres, 102, 13 019–13 035, https://doi.org/https://doi.org/10.1029/97JD00901, 1997.

World Meteorological Organization (WMO): Scientific Assessment of Ozone Depletion: 2018, Tech. Rep. 58, World Meteorological Organisation Global Ozone Research and Monitoring Project-Report No. 58, Geneva, Switzerland, http://ozone.unep.org/science/assessment/sap, 2018.

World Meteorological Organization, (WMO): Executive Summary. Scientific Assessment of Ozone Depletion: 2022, Tech. Rep. 278, WMO, Geneva, 2022.

Young, P. J., Harper, A. B., Huntingford, C., Paul, N. D., Morgenstern, O., Newman, P. A., Oman, L. D., Madronich, S., and Garcia, R. R.: The Montreal Protocol protects the terrestrial carbon sink, Nature, 596, 384–388, https://doi.org/10.1038/s41586-021-03737-3, 2021.